FETMA: A Simple Code for Thermo-Mechanical Analysis on BWR Fuel Rods

Hector Hernandez-Lopez

Nuclear System Department, National Institute for Nuclear Research
Carr. Mexico-Toluca s/n (km 36.5), La marquesa, Ocoyoacac, Mexico, 52750
hector.hernandez@inin.gob.mx

***Abstract*- The new designs of fuel elements are enhanced to reach high burn-up. If these new designs can satisfy the safety design constraints, a strong positive economic impact can be achieved. Thus, for safety and economic evaluations, the behaviour of fuel elements needs to be analysed. A computational tool was developed to analyse the thermo-mechanical behaviour of current new design fuel elements during normal or transient operation. This computational code solves the diffusion equation with six neutron energy groups, so the influence of fast neutrons on the cladding can be better estimated. Fuel depletion, not considering the gadolinium as burnable poison, calculations for fission product yield is also performed. A description of the code and result obtained are presented in this task.**

Keywords- Thermo-mechanical; Fuel Rods; BWR; Code

I. INTRODUCTION

In the nuclear industry, the new fuel assembly designs are continuously under development. These designs are submitted to high burn-up and long residence time inside the core of the nuclear reactor, as is the case of Laguna Verde Nuclear Power Plant (LVNPP). The new designs should provide warranty to satisfy high safety levels, given that a fuel failure plays an important role in safety when the economic impact is too high. The nuclear fuel manufacturer evaluates their designs to warrant the safety of the Nuclear Power Plant. However, due to safety and economic topics, the behaviour of fuel elements needs to be analyzed during its life inside the reactor core. In the National Institute for Nuclear Research (ININ, Instituto Nacional de Investigaciones Nucleares), a computational tool was developed to analyse the thermo-mechanical behaviour of current new designs of fuel elements during normal or transient operation to be used at LVNPP.

The aim of this task is to develop a computer code for fuel elements thermo-mechanical analysis for assessing the fuel elements performance normal and transient operation. This code considers that different phenomena will occur at a fuel element when introduced into a power reactor. These phenomena are due to fission, a chemical and physical process. The processes of heat and mass transport that occur as a result of heat are generated by fission, and chemical reactions that occur between the materials are from fuel, cladding and coolant.

The code is divided into three parts: neutronic, thermal and mechanical. From a difference respect to other codes, the FETMA code evaluates all aspects involved in fuel element performance inside reactor core, and takes into account several operation conditions at present. The sequence of calculation employed by the FETMA code is shown in Fig. 1.

The neutron microscopic cross section library for six energy neutron groups contains 19 isotopes including material components of fuel rod and 4 main fission products. The one dimension, axial direction, diffusion equation in six energy groups is approximated considering fuel homogenization by node. The fuel rod power calculation is made taking into account its position in the fuel assembly and location in the reactor core. Also, burn-up and production of fission products are calculated.

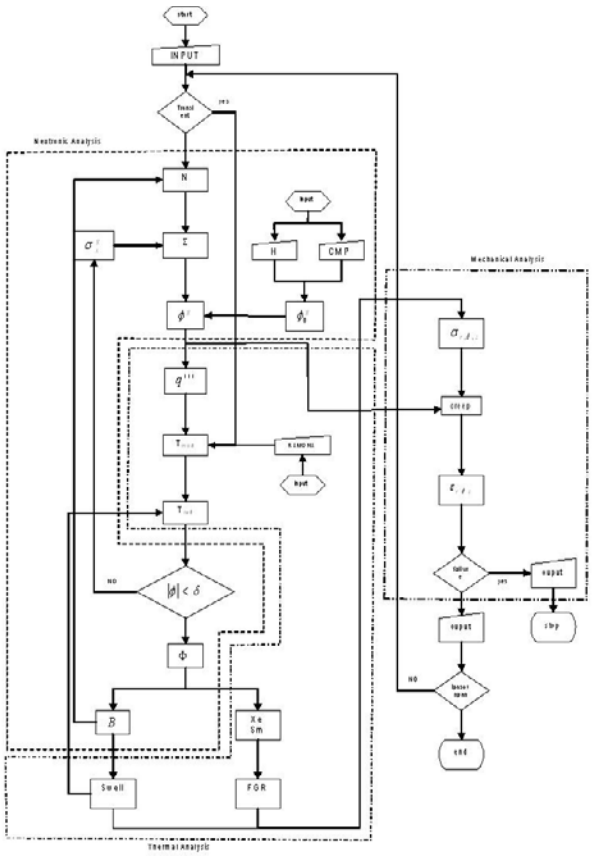

Fig. 1 Sequence of calculation employed by FETMA code

The first approach employs neutron flux from the axial power distribution obtained by CM-PRESTO [1] for the assembly where the fuel rod is located, CM-PRESTO ensemble average values reported by the additional use of HELIOS code [2] to obtain the radial distribution in fuel lattice. HELIOS takes into account the presence or absence of the control rod and the voids ratio at which the fuel lattice

is considered to produce a search that implicitly takes into account these considerations.

The axial temperature distribution in coolant channel and one or two phases along the channel are approximate. In this case it is necessary to execute calculations about void and steam quality distributions, as well as pressure drop in the coolant channel. The calculations for radial temperature distribution in the fuel rod are executed considering fuel density changes and gas volume is increased into the gap.

Finally, the stresses and strains distribution is caused by temperature changes and materials that affect both the fuel and cladding, causing the phenomena of densification and creep. The stresses and strains distributions is caused purely by mechanical phenomena because of pellet-cladding interaction and changes in the internal pressure due to fission gas released from the pellet to gap. By assessment, the effects are caused by radiation to fuel, which is the result of swelling suffered by the pellets due to accumulation of fission gas, as well as cladding, which is presented as the creep of the material product of the neutron irradiation.

II. NEUTRONIC ANALYSIS

A. Microscopic Cross Sections

To generate the microscopic cross section library, the NJOY code [3] was used and the database ENDF-B/IV-rel 4. [4], the library generation are obtained by the application of the modules contained in the NJOY code, as shown in Fig. 2.

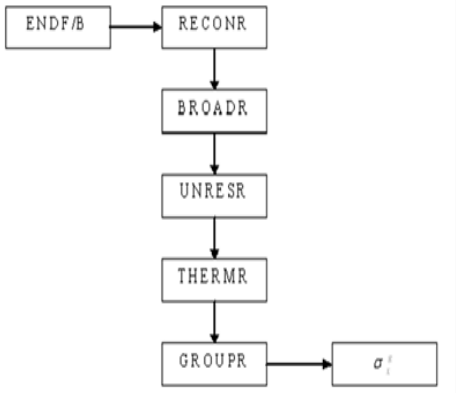

Fig. 2 Sequence used in NJOY for calculation of microscopic cross sections

The library is obtained after the reconstruction of parameters of resonance, characterization of the Doppler widening at high temperatures and energy losses, calculation of the self-shielding in the region of unresolved resonances, generation of the dispersion effective sections in the thermal energy interval, and finally the processing of the sections by energy group.

Table 1 shows the energy groups considered in FETMA. These energy cuts are taken from Stammler [5]. Similarly, Table II shows the isotopes included in the library of cross sections for FETMA. As it can be seen, it includes data for the coolant, cladding, fission products, poisons, burnable poisons, fuel and plutonium.

TABLE I ENERGY GROUPS AND LETHARGY USED IN FETMA CODE

Group	E_{min} [eV]	E_{max} [eV]	U
6	1.x10-6	0.625	18.16
5	0.625	4	16.05
4	4	9.877	14.66
3	9.877	$9.118x10^3$	12.66
2	$9.118x10^3$	$0.821x10^6$	6.899
1	$0.821x10^6$	$1.x10^7$	1.435

TABLE II MICROSCOPIC CROSS SECTION ISOTOPES LIBRARY CONTAINED IN FETMA CODE

^{1}H	^{149}Pm	^{157}Gd	^{239}Pu
^{16}O	^{149}Sm	^{158}Gd	^{240}Pu
Zr-nat	^{154}Gd	^{160}Gd	^{241}Pu
^{135}I	^{155}Gd	^{235}U	^{242}Pu
^{135}Xe	^{156}Gd	^{238}U	

B. Neutron Diffusion

FETMA resolves the diffusion equation in a system of six differential equations coupled with six unknowns; therefore, to make the spatial discretization we are using, the cash method of integration is based on finite differences. In order to solve the system, it applies the Gauss-Seidel iterative method, as shown in the following Equation (1).

$$\begin{aligned}
&-\nabla D_1(z)\nabla\phi_1(z)+\Sigma_{R_1}\phi_1(z)=\frac{1}{\lambda}\chi_1\sum_{i=1}^{6}\nu_i(z)\Sigma_{fi}(z)\phi_i(z)\\
&-\nabla D_2(z)\nabla\phi_2(z)+\Sigma_{R_2}\phi_2(z)=\frac{1}{\lambda}\chi_2\sum_{i=1}^{6}\nu_i(z)\Sigma_{fi}(z)\phi_i(z)+\Sigma_S^{1\to2}(z)\phi_1(z)\\
&-\nabla D_3(z)\nabla\phi_3(z)+\Sigma_{R_3}\phi_3(z)=\frac{1}{\lambda}\chi_3\sum_{i=1}^{6}\nu_i(z)\Sigma_{fi}(z)\phi_i(z)+\Sigma_S^{1\to2}(z)\phi_1(z)+\Sigma_S^{2\to3}(z)\phi_2(z)\\
&\vdots\\
&-\nabla D_6(z)\nabla\phi_6(z)+\Sigma_{R_6}\phi_6(z)=\frac{1}{\lambda}\chi_6\sum_{i=1}^{6}\nu_i(z)\Sigma_{fi}(z)\phi_i(z)+\Sigma_S^{1\to2}(z)\phi_1(z)+\cdots+\Sigma_S^{1\to5}(z)\phi_5(z)
\end{aligned} \tag{1}$$

C. Fuel Burn-up

During the operation of a nuclear reactor for fuel material composition, it will change as the fissile isotopes are consumed and fission products are produced. This process can be monitored over the lifetime of the reactor in an effort to determine the material composition and reactivity as a function of the energy released. This requires the depletion and production chains for the main isotopes, ^{235}U and ^{238}U, coupled with the equations that determine the neutron flux in the reactor core. On the other hand, the schemes that continuously estimate the content of fission products such as ^{135}Xe, ^{149}Pm and ^{149}Sm. observed the importance of ^{135}I, ^{135}Xe for both neutron and for the mechanical performance. A good approximation is needed for the volume that would come to occupy within the fuel rod.

Both fission products and isotopes that make nuclear fuel follow the pattern of generation-consumption are mathematically detailed in Equation (2).

$$\frac{dN_A}{dt}=-\lambda_A N_A-\left[\sum_g\sigma_{a_g}^{A}\phi_g\right]N_A+\lambda_B N_B+\left[\sum_g\sigma_{a_g}^{C}\phi_g\right]N_C \tag{2}$$

Where: $N_{A,\,B,\,C}$ is the isotopic density A, B and C isotopes. $\sigma_{A,C}$ is the microscopic cross section of absorption of isotopes A and C. $\lambda_{A,B}$ is the decay constant of isotope A and B.

III. TEMPERATURES DISTRIBUTION

A. One Phase

In boiling water reactors (BWR), the coolant temperature, along with the fuel rod should be studied in two physical regions. The first occurs when water maintains its liquid phase: hz<hsat. The change of temperature along the water channel considers the enthalpy as a function of system pressure and it should be based on drop pressure due to friction in the channel, pressure hydrostatics, and the form of the channel.

The coolant's density and temperature are determined as a function of enthalpy (h) and pressure (p). In the region where coolant is boiling, ($h_i > h_{SAT}$ or $z_i > z_{SBC}$), the temperature is found in the balance equation. The pressure drop is modified due to two phases flow effects. Changes in water temperature along the cooling channel are given by Equation (3).

$$h_{i+1} = h_i + \frac{\Delta z}{2w}\left(q_i + q_{i+1}\right) \tag{3}$$

where: q is the rate of heat generation [W]. *w* is the mass flow of refrigerant [kg / sec]. Δz is the difference in height of the node [m]. h_i is the enthalpy in the ith node [kJ / kg].

Where the enthalpy h is a function of system pressure at z, therefore variations in system pressure due to friction ΔPf, the hydrostatic ΔPh and ΔPF channel shape must be considered; system pressure at z is defined by Equation (4) [6].

$$P_i = P_{i-1} - \frac{2\Delta z_i}{D_h}\rho_i \overline{u_{z_i}^2} f\left(\mathrm{Re}_i\right) - \rho_i g \Delta z_i - \sum_i \frac{K_i \rho_i \overline{u_{z_i}^2}}{2} \tag{4}$$

where: P_i is the pressure in the coolant channel at point i [Bar]. D_h is the equivalent diameter of the fuel rod analyzed [dimensionless]. $f_{(Re)}$ is the fanning friction factor as a function of Reynolds number and relative roughness [-]. Re is the Reynolds number, calculated for a fluid with forced circulation [-]. ρ_i is the density of the refrigerant at point i [Kg/m3]. K_i is a friction factor determined for each type of grid spacer. g is the gravitational constant [9.8 m/s2]. u_z^2 is the square of the average velocity of the refrigerant at point i [m / s].

Once you have determined the enthalpy, it defines the density and temperature of the coolant as a function of h and P using the correlations published by Jordan [7].

B. Two Phases Flow

This is a regional characteristic of reactors cooled by boiling light water (BWR), which presents the boiling of coolant, $h_i = h_{sat}$ where, in order to find the temperature of the system, is part of the energy balance equation, which gives us the enthalpy at each point of the channel. The pressure drop is modified according to the effects of two-phase flows; these changes are implemented into the Martinelli-Nelson correlation [8] for the pressure drop due to friction, see Equation (5).

$$\Delta P_i^f = \left[\Delta P_i^f\right]_f R_{MN} \tag{5}$$

where: ΔP_i^f is the pressure drop in one phase, at the point z_i. R_{MN} is the Martinelli-Nelson multiplier, depending on the pressure and the quality of the coolant at point z_i.

Moreover, the pressure drop by the acceleration ΔPa has to be taken account of and has the following form, see Equation (6).

$$\Delta P_i^a \approx \rho_i \overline{u_{z_i}^2}\left[\frac{r_i - r_{i-1}}{\Delta z_{i-1}}\right]\Delta z_i \tag{6}$$

where: α is the fraction of voids in the coolant. ρ_l is the density of the refrigerant in its liquid phase. ρ_g is the density of the refrigerant in its gaseous phase

Once the system pressure is found, the correlations are applied; it is developed by Saul [9] to find h_g, h_l, ρ_l, ρ_g.

In addition to T_{sat} $T_i = (P_i)$.

C. Radial Temperature Distribution

The energy transport equation describes the temperature distribution in a solid, which is assumed to be incompressible and with negligible thermal expansion. Also a steady state is assumed so that the resolved expression for the temperature distribution in the radial direction is given by Equation (7).

$$-\nabla \cdot k\left(\vec{r},T\right)\nabla T\left(\vec{r}\right) = q'''\left(\vec{r}\right) \tag{7}$$

where: $k\left(\vec{r},T\right)$ is the coefficient of thermal conductivity as a function of position and temperature.

For purposes calculation, one can consider the surface temperature of the cladding as a reference temperature; it will be determined in terms of coolant temperature. To simplify the calculations, certain assumptions were made.

We assume that one can neglect thermal conduction in the axial direction; this is because temperature gradients in the radial direction are greater by several orders of magnitude to gradients in the axial direction. As the heat transfer in the axial direction will take place outside of the fuel by the coolant through forced circulation. The fission energy appears as a uniform heat source distributed through the combustible material; usually there is some variation in the heat source because it is proportional to the neutron flux in the fuel. Only the heat transfer is considered in steady state.

Given these assumptions, for the implementation of Equation (7) in the temperature analysis, the different coefficients of thermal conductivity must consider, as presented in the fuel materials, i.e, the thermal conductivity of the pellet fuel, thermal conductivity, which occurs in the pellet-cladding gap and the thermal conductivity through the cladding.

FETMA code contemplates the use of four models to represent the coefficient of thermal conductivity, which are functions of density, burn-up and amount of gadolinium. The first model to calculate the thermal conductivity is taken from the properties of nuclear materials covered MATPRO Version 9 [10]. The second model is determined from experimental data obtained in the reactor HALDEN

[11]. The third model includes dependence on the density and temperature of the fuel, which was developed by Lucuta [12]. The final model considers a dependency on the content of gadolinium in the fuel pellet developed by Fukushima [13]. Fig. 3 shows the behavior of models of UO2 thermal conductivity used in FETMA code.

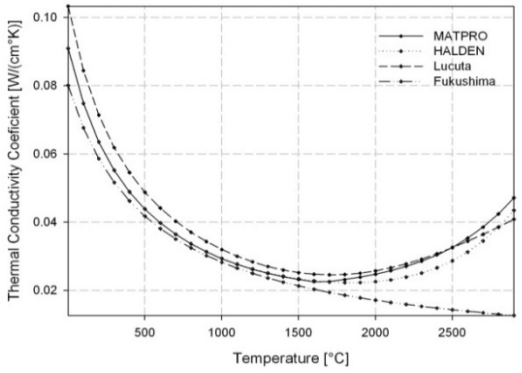

Fig. 3 Models of UO2 thermal conductivity used in FETMA code

D. Thermal Conductance Gap

Since some fuel rods use He or other gas to fill the clearance between combustible material and the cladding, the heat transfer model through it should consider the conductance through the gas and thermal radiation between surfaces, combustible material and cladding. In addition to heating and irradiation, swelling occurs in fuel material, which can produce contacts between fuel and cladding.

Since the problem of determining the conductance in the clearance (hgap) is very difficult to resolve by the number of variables that are involved in design, hgap is considered 1 W/m2°K. However, there are relationships which may give a more realistic approximation of the value of hgap; in our case we take a model proposed by Ross and Stoute [14].

E. Cladding

To calculate the temperature of the cladding, the coefficient of thermal conductivity of zircaloy is considered so that Anderson [15] evaluates test data and adjust minimum through a cubic equation in terms of temperature. Equation (8) can be applied both to zircaloy-2 and zircaloy-4, as the fit of the data was carried out with data from both alloys.

$$k(T) = 7.151 + 2.472x10^{-3}T + 1.674x10^{-6}T^2 - 3.334x10^{-10}T^3 \qquad (8)$$

where: T is the temperature in the cladding [°K]. K is the coefficient of thermal conductivity [W/m°K].

IV. THERMAL-MECHANICAL STRESS

A. Fuel Strain

In the case of the ceramic fuel, the problems of thermal stress are of primary importance. In general, ceramics have little ductibility compared with metallic materials, and therefore are more fragile. Thus, the fuel rods are subject to another type of stress, which is produced by swelling in the pellet and material creep. This stress should be considered in the mechanical analysis of the fuel rod.

Equation (9) shows the model used for calculating the deformation ε in terms of stress σ, in cylindrical coordinates.

$$\varepsilon_r = \frac{1}{E}\left[\sigma_r - \upsilon(\sigma_\theta + \sigma_Z)\right] + \varepsilon_{cr} + \varepsilon_{sw} + \varepsilon_{th}$$

$$\varepsilon_\theta = \frac{1}{E}\left[\sigma_\theta - \upsilon(\sigma_r + \sigma_Z)\right] + \varepsilon_{cr} + \varepsilon_{sw} + \varepsilon_{th} \qquad (9)$$

$$\varepsilon_z = \frac{1}{E}\left[\sigma_z - \upsilon(\sigma_\theta + \sigma_r)\right] + \varepsilon_{cr} + \varepsilon_{sw} + \varepsilon_{th}$$

where: ε_i is the strain in the direction i (r, θ, z) [m / m]. σ_i stress in the direction i (r, θ, z) [MPa]. E is Young's modulus [MPa]. ν is the Poison's modulus [dimensionless]. ε_{cr} is caused by creep deformation [m / m]. ε_{sw} is the strain caused by swelling [m / m]. ε_{th} is the deformation due to thermal expansion, given by αT [m / m]. A is the thermal expansion coefficient [m / (m ° C)].

It should be noted that strain due to creep, swelling and thermal expansion does not depend on the position and can be considered constant. To solve this we must assume that the axial deformation of the fuel is absorbed by the springs that hold the fuel inside the bar.

Cladding of the thermal stress is due to an expansion produced by a differential temperature between the inner and external walls of the rod. The region inside the cladding, near the fuel, is hotter than the external region, which causes compression stress near the inside face and tensile stress near the external face of the cladding.

The stresses, due to pressure, are the result of the pressure difference between inside and outside of the fuel rod. The external pressure is caused by the pressure of system operation, while the internal pressure is caused by the expansion of the gas-filled rod and the release of fission gases as a result of irradiation.

B. Sweeling

During the same process of burning a fuel, each fission atom is replaced by two fission product atoms, with about half the atomic weight of the fissionable atom each. Of these atoms, about 15% are inert gases, such as Xe and Kr, and the remaining are solids and soluble gaseous oxygen.

Once the initial densification is completed, the fuel tends to swell as the burn-up is increasing. This phase of swelling is sometimes less pronounced at lower densities, i.e, a greater number of pores in the material versus a combustible material with fewer pores, which represents a higher density.

At specific temperatures and operation levels due to the degree of burn-up of a light water reactor, the fuel-swelling ratio has a value of approximately 0.5% of volume per 10^{20} fissions per cubic centimeter of fuel material, approximately 4.15 GWD/TMU (10.GWD/TMU = $2.41x10^{20}$ fissions/cm^3).

The volume change caused by non-gaseous fission products is very difficult to measure; however, there had been many experiments to establish relative amounts, taking into account the elements and compounds produced. The

code makes use of the model described by Equation (10), proposed by [16, 17].

$$\left(\frac{\Delta V}{V}\right)_{sol} = 7.435x10^{-3}\rho\left(B_1 - B_0\right) \quad (10)$$

where: B_i is burn-up in a time step i [MW/KgU]. P is the initial density of fuel material [kg/m^3]. $\left(\frac{\Delta V}{V}\right)_{sol}$ is the fraction of change in volume due to solid fission products.

The swelling due to fission gases is caused by the increased number of bubbles of gas produced; however, the physical mechanisms that cause it are too complex. As in the swelling caused by solids, gaseous products are calculated by an experimental correlation; Equation (11) expressed in terms of temperature and burn-up of the fuel pellet [18, 19].

$$\left(\frac{\Delta V}{V}\right)_{gas} = 2.617x10^{-39}\rho B(2800 - T)\exp[-0.0162(2800 - T)]\exp(-2.4x10^{-10}\rho B) \quad (11)$$

where: T is the average fuel temperature [°K]. B is burned in a time step [MW/KgU]. P is the initial density of fuel material [kg/m3]. $\left(\frac{\Delta V}{V}\right)_{gas}$ is the fraction of change in volume due to gaseous fission products.

Therefore, the swelling caused by the pellet fuel fission products is the sum of both cases [20].

On the other hand, the swelling that occurred in the cladding is approximated by the model used by Benjamin [21] in the code ISUNE2 and is described by Equation (12).

$$\left(\frac{\Delta V}{V}\right) = 9\times10^{-35}\left(\phi\cdot t\right)^{1.5}\times \left(4.028 - 3.712\times10^{-2}T + 1.0145\times10^{-4}T^2 - 7.879\times10^{-8}T^3\right) \quad (12)$$

where: T is the average temperature in cladding [°C]. T is the irradiation time [seg]. ϕ is the fast neutron flux with energies > 1 MeV. [n/cm^2-seg]

C. Fission Gas Release

As mentioned above, as a result of the ^{235}U fission, the Xe is produced, an insoluble inert gas in the fuel matrix can be contained within the fuel matrix causing swelling of the matrix, or else be released to the cavities forming the fuel cladding gap and the central void of the tablet, if any, through the cracks that are formed within the fuel element and connecting pores too large, with the above mentioned regions.

However, only a fraction of these Xe atoms produced, manage to escape to these areas, thereby producing an increase in filling gas pressure that is within the recoil, which has a direct impact on the tensions experienced by the fuel cladding.

The fractions of gas release are very difficult to measure; however, several experimental measurements support that these quantities are evaluated by the model proposed by [22].

D. Creep

Creep is the tendency of a solid material to slowly move or deform permanently under the influence of stresses. It occurs as a result of long term exposure to levels of stress that are below the yield strength of the material. Creep is more severe in materials that are subjected to heat for long periods and near the melting point. Creep always increases with temperature.

The rate of this deformation is a function of the material properties, exposure time, exposure temperature and the applied structural load. Depending on the magnitude of the applied stress and its duration, the deformation may become so large that a component can no longer perform its function. Creep is usually of concern to engineers and metallurgists when evaluating components that operate under high stresses or high temperatures. Creep is a deformation mechanism that may or may not constitute a failure mode. Moderate creep in concrete is sometimes welcomed because it relieves tensile stresses that might otherwise lead to cracking.

Unlike brittle fracture, creep deformation does not occur suddenly upon the application of stress. Instead, strain accumulates as a result of long-term stress. Creep deformation is a "time-dependent" deformation.

In some materials, especially polycrystalline like UO_2, creep approaches a continuous distribution of modes of sliding points of the lattice dislocation. In this case, incorporating the model more accurately represents the phenomenon of creeping, which was originally proposed by Bohaboy [23] and modified by Solomon [24] as shown in Equation (13), and it is actually used for other codes.

$$\dot{\varepsilon}(T) = \frac{\left(A_1 + A_2\dot{F}\right)\sigma_{trans}\exp\left(-\frac{Q_1}{RT}\right)}{\left(A_3 + D\right)G^2} + \frac{A_4\sigma_{trans}^{4.5}\exp\left(-\frac{Q_2}{RT}\right)}{A_6 + D} + A_7\sigma_{trans}\dot{F}\exp\left(-\frac{Q_3}{RT}\right) \quad (13)$$

Where:

A_1= 3.919x10^5

A_2=1.305x10^{-13}

A_3= -87.7

A_4= 203.7

A_6= -90.5

A_7= 3.723x10^{-29}

Q_1= 376,740 (J/mol)

Q_2= 552,552 (J/mol)

Q_3= 21,767 (J/mol)

σ_{trans}=165.5 G$^{-0.5714}$

R= 8.314 (J/mol°K)

T is the temperature (°K)

D is the density fraction between [0.92, 0.98]

G is the grain size ~ 30 µm

The cladding creep model that was proposed by Ibrahim [25] is given by Equation (14).

$$\varepsilon_{cr} = \sqrt{t}\left[5.7\times10^{-12}\left(1 + 1.0\times10^{8}T^{-7}\phi^{0.65}\right)\left(\sigma_{eff} + 710.0e^{4.97\times10^{-8}\sigma_{eff}}\right)\cdot e^{\left(-\frac{42000}{RT}\right)}\right] \quad (14)$$

where: T is the irradiation time [seg]. ϕ is the fast neutron flux with energies > 1 MeV [1/cm^2-seg]. T is the average temperature in the cladding [ºK]. σ_{eff} is the effective stress in the cladding [Pa]. R is the ideal gases constant.

V. VALIDATION OF CODE

In order to verify the results provided by code FETMA, an exercise was made by which the corresponding data to the distribution of the neutron flux were observed, as well as the fuel center temperatures, the fraction of fission gases released to gap and the elongation of the cladding. In Table III, the data used for the verification exercise can be found.

TABLE III PARAMETERS USED IN EXERCISE OF FETMA CODE VERIFICATION

Enrichment ^{235}U	3.38 $^{w}/_{0}$
Pellet Diameter	1.0439 cm
Internal Cladding Diameter	1.0650 cm
External Cladding Diameter	1.2250 cm
Pitch	1.6256 cm
Density	96.5%
Size grain	7.83 µm
Feedwater Temperature	286 °C
System Pressure	70 Bar
Coolant Flow	1400 kg/(m^{2}s)

Fig. 4 shows the neutron flux behavior for energy group higher than 0.821 MeV, whereas Fig. 5 shows the neutron flux behavior for energy group less than 0.625 eV, being observed that the flux represents the behavior of the power distribution.

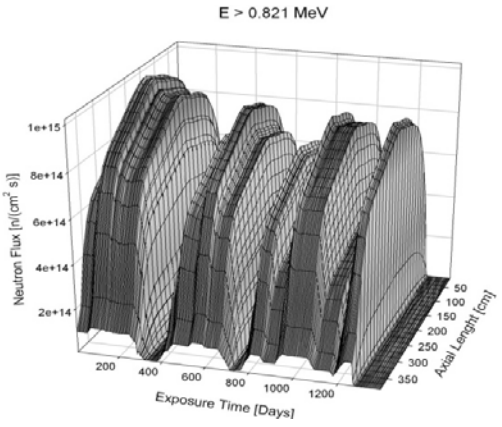

Fig. 4 Neutron flux for energy more than 0.821 MeV evaluated for FETMA

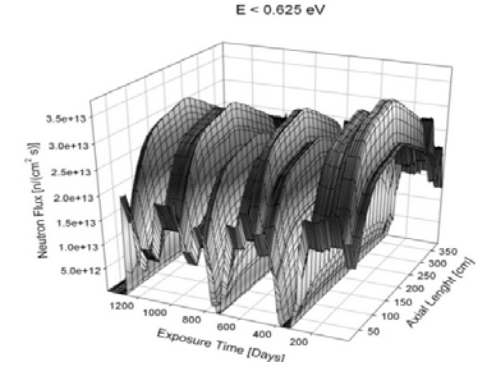

Fig. 5 Neutron flux of energy less than 0.625 eV evaluated for FETMA

To verify the capability of thermal analysis of FETMA, code calculation has been compared with the data of fuel center temperature within experiment IFA-597.2 [26]. The data set covers the temperature vs. power for Rod 8 during the first 4 ramps. Fig. 6 shows a comparison between the FETMA calculations and measurements of fuel center temperature. Fig. 7 shows the fuel center temperature behavior as function of the linear heat rate.

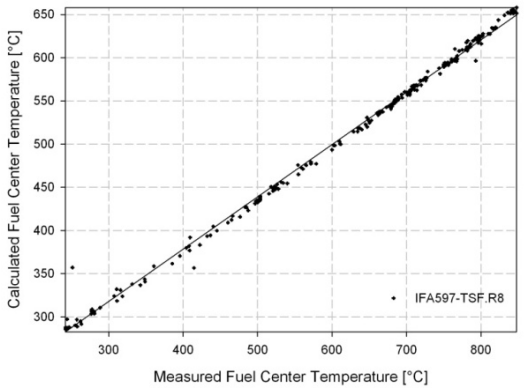

Fig. 6 Comparison between measured and calculated temperatures of fuel centerline

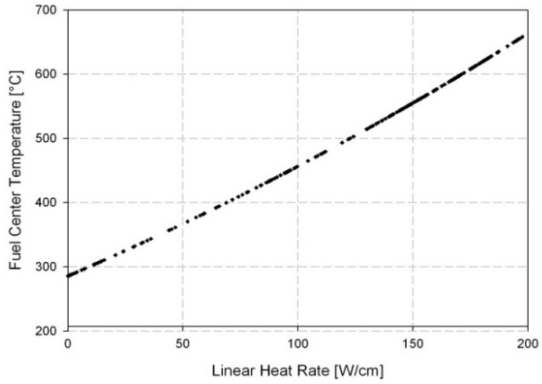

Fig. 7 Temperature at fuel centerline during power increase

To verify the capability of the FETMA code and to calculate the fission gas release, the fission gas release behavior during irradiation has been observed in Fig. 8 and it shows good agreement with the theory.

In order to verify the capability of global mechanical analysis of FETMA, the calculations of cladding elongation during first four ramps is shown in Fig. 9.

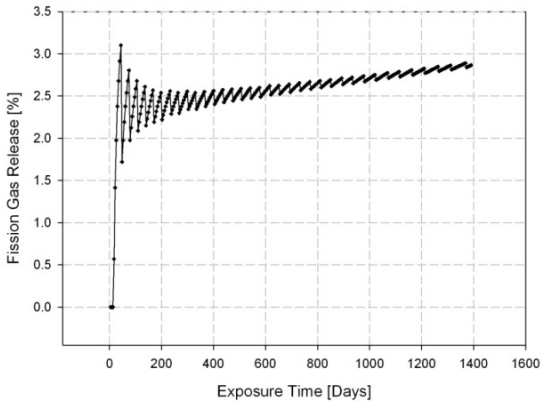

Fig. 8 Fission gas release calculated during exposure time

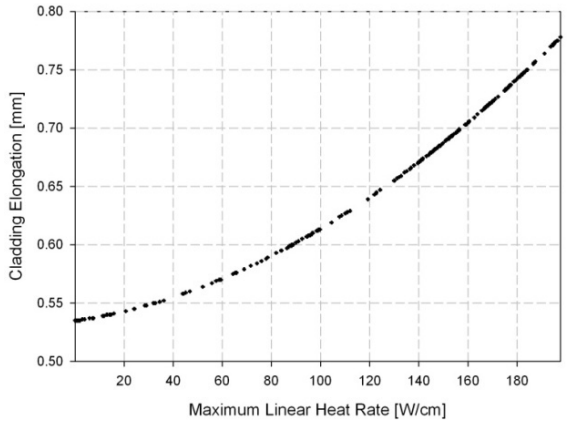

Fig. 9 Cladding strain as function from maximum power during power increase

VI. CONCLUSIONS

A fuel behavior model in code FETMA has been developed for the analysis of neutronic, thermal and mechanical behavior of boiling water fuel rod during steady-state and transient conditions. The capability of FETMA has been verified using some data base obtained in the NEA Data Bank. The results of comparison between FETMA calculations and experimental data for fuel center temperature showed that the agreement was satisfactory. Other parameters were just evaluated theoretically. However, the results obtained with FETMA were consistent with theoretical results.

REFERENCES

[1] Scandpower 1996 CM-PRESTO User Manual.

[2] Scandpower 1999 HELIOS User Manual.

[3] R. E. MacFarlane & D. W. Muir, The NJOY Nuclear Data Processing System, Version 91. LA-12740-M, October 1994.

[4] G M Hale, P G Young, "ENDF/B-IV", Los Alamos National Laboratory, 2000.

[5] R. J. J. Stamnn´ler, Methods of Steady-State Reactor Physics in Nuclear Design, Academic Press, 1983.

[6] J. Duderstadt and L. Hamilton, Nuclear Reactor Analysis, John Wiley and Sons, Inc., 1976.

[7] R. E. MacFarlane & D.W. Muir, The NJOY Nuclear Data Processing System, Version 91. LA-12740-M, October 1994.

[8] W. B. Jordan, Addendum to Fits to Thermodynamic Properties of Water, KAPL-m-6734, Knoll Atomic Power Lab., N. Y. USA. 1968.

[9] Martinelli, R. C. Nelson, D.B., "Prediction of Pressure Drop During Forced Circulation Boiling of Water", Transactions of ASME, 695-702, 1948.

[10] Saul and W. Wagner, IAPWS Formulation 1995 for the Thermodynamic Properties of Ordinary Water Substance for General and Scientific Use, to be published in J. Phys.Chem.Ref. Data, 1999.

[11] MATPRO-09, A Handbook of Materials Properties for Use in the Analysis of Light Water Reactor Fuel Rod Behavior, USNRC TREE NUREG-1005, 1976.

[12] Weisenack, W., et al., HWR-469, 1996.

[13] Lucuta P. G., APragmatic Approach to Modelling Thermal Conductivity of Irradiated UO2 Fuel, J. Nuclear Materials 232, pp166-180, 1996.

[14] Fukushima S., Ohmichi T., Maeda A., and Watanabe H., The Effect of Gadolinium Content on the Thermal Conductivity of Near-Stoichiometric (U,Gd)O2 Solid Solutions, ibid 105, pp201-210, 1982.

[15] M. Ross and R. L. Stoute, Heat Transfer Coefficient between U02 and Zircaloy-2, AECL-1552, Chalk River, Ontario, Canada, June 1962.

[16] W. K. Anderson, C. J. Beck, A. R. Kephart, J. S. Theilacker, Zirconium Alloys Reactor Structural Materials: Engineering Properties as Affected by Nuclear Reactor Service, ASTM-STP-314 , pp 62-93,1962.

[17] F. Anselin, The Role of Fission Products in the Swelling of Irradiated U02 and (U, Pu) 02 Fuel, EAP-5583, January 1969.

[18] T. C Rowland, M, O. Marlowe, R. B. Elkins, Fission Product Swelling in BWR Fuels, NEDO-20702, November 1974.

[19] J. A. Turnbull, The Effect of Grain Size on the Swelling and Gas Release Properties ofU02 During Irradiation, Journ. Nucl. Mat., 50, pp 62-68, 1974.

[20] W. Chubb, V. W. Storhok, and D. I. Keller, Factors Affecting the Swelling of Nuclear Fuel at High Temperatures, Nuclear Technology, 18 pp 231-255, June 1973.

[21] D. Olander, Fundamental Aspects of Nuclear Reactor Fuel Elements, Technical Information Center, ERDA, 1976.

[22] Benjamin, M. MA., Irradiation Swelling, Creep, and Thermal-Stress Analysis of LWR Fuel Elements, Computer Code ISUNE-2, Nuclear Engineering and Design 34, pp 361-378, 1975.

[23] Weisman, J., et al, Fission Gas Release from UO2 Fuel Rods with Time Varying Power Histories, Transactions of the American Nuclear Society,, 12, pp 900-901, 1969.

[24] Bohaboy, P., et al, Compressive Creep Characteristics of Ceramic Oxide Nuclear Fuels: Part I: Uranium Dioxide, Presented at American Ceramic Society Nuclear Division, Pittsburgh, Pennsylvania, October 6-8, 1968.

[25] Solomon, A., et al, Fission Induced Creep of UO2 and its Significance to Fuel Element Performance, LANL-7857, September 1971.

[26] Ibrahim, E., In-Reactor Creep of Ziconium-Alloy Tubes and its Correlation with Uniaxial Data, applications-Related Phenomena for Zircaloy and its Alloys, ASTM-STP-458, Philadelphia, American Society for Testing and materials, pp 18-36, 1969.

[27] IFPE/IFA-597.3, Center-line temperature, fission gas release and clad elongation at high burnup (60-62 MWd/Kg), NEA, 1985.

Hector Hernandez-Lopez: Bachelor in Science by School of Physics and Mathematics from National Polytechnic Institute, 1992. Master in Nuclear Science by Faculty of Chemistry from National Autonomous Mexico University, 1997; Doctor in Nuclear Science by Faculty of Sciences from University Autonomous of State of Mexico, 2009.

Since 1992 he has been working in Nuclear Systems Department of National Institute for Nuclear Research in nuclear fuel management performing simulations in steady-state for reactors of Laguna Verde Nuclear Power Plant. In the last ten years he has dedicated to thermo-mechanical analysis of fuel elements of boiling water reactors.